Available *online* at : http://jnte.ft.unand.ac.id/

Jurnal Nasional Teknik Elektro

| ISSN (Print) 2302-2949 | ISSN (Online) 2407-7267 |

Comparative Analysis of Two-Stage and Single-Stage Models in Batteryless PV Systems for Motor Power Supply

I Wayan Sutaya [1], Ida Ayu Dwi Giriantari [2], Wayan Gede Ariastina [3], I Nyoman Satya Kumara [4]

[1] Electronics Systems Engineering Technology Department, Universitas Pendidikan Ganesha, Jl. Udayana No.11, Singaraja, Bali, 81116, Indonesia
[2,3,4] Electrical Engineering Department, Universitas Udayana, Jln. P.B.Sudirman, Denpasar, Bali, 80234, Indonesia

ARTICLE INFORMATION

Received: December 23, 2023
Revised: February 10, 2023
Accepted: February 25, 2023
Available online: March 29, 2023

KEYWORDS

Photovoltaic Systems, Maximum Power Point Tracking (MPPT), Two-Stage Model, Single-Stage Model, Motor Power Consumption

CORRESPONDENCE

Phone: +6281236777971

E-mail: wsutaya@undiksha.ac.id

A B S T R A C T

Implementing photovoltaic (PV) systems as direct power sources for motors without batteries is a complex process that requires a sophisticated control mechanism. The crucial aspect of PV systems is the Maximum Power Point Tracking (MPPT) process, which ensures that the installed PV system generates optimal energy output. A recent study has analyzed research related to PV systems supplying power to pump motors, and the results have successfully classified these systems into two main models: the two-stage and the single-stage. The two-stage model involves separate power tracking and load consumption control processes, while the single-stage model integrates power tracking and load consumption control into a single process. A comparative analysis of these two models has revealed that the two-stage model exhibits higher stability due to the separate power tracking and load consumption control processes. Aspects such as the MPPT process, motor power consumption, and the utilization of DC-link capacitors were examined in this study. The findings of this comparative study contribute valuable insights into the effectiveness and stability of two-stage and single-stage models in PV systems supplying power to motors without batteries. The results will significantly interest researchers and practitioners working in Photovoltaic systems and motor control, providing helpful information for designing and implementing more efficient and reliable PV systems.

INTRODUCTION

Photovoltaic (PV) power's successful integration relies on showcasing economic superiority over fossil fuel electricity. A promising approach is the direct use of PV systems to power pump motors without batteries. It primarily benefits agricultural irrigation with its synchronous energy demand and PV availability [1]. This adaptable system is also applicable to water supply companies managing reservoirs [2], dynamically adjusting pumping operations based on the feasibility of PV power production. This streamlined utilization underscores the efficiency and potential of PV systems in diverse settings.

The electrical power generated by PV systems can drive electric motors for various industrial applications. However, a notable challenge with PV lies in its reliance on fluctuating sunlight. Consequently, the power output of PV systems also fluctuates. Therefore, PV systems for driving pump motors are well-suited for variable speed applications[3].

Directly driving motors using PV systems necessitates creative design and solutions to address challenges stemming from varying and limited power, aiming to maximize both the energy produced by PV and the volume of pumped water. Within these PV systems, induction motors serving as pump drivers exhibit superior performance compared to others due to their productivity, reliability, low maintenance requirements, and cost-effectiveness [4].

The most significant potential for utilizing this PV system lies within power generation companies. This system involves storing electrical energy in the form of water within reservoirs. Subsequently, when needed, this water is utilized to drive power generator turbines, ensuring energy reliability without using batteries. In this setup, solar-derived electricity is stored as mechanical energy in water held in a higher-positioned reservoir [5].

The cost of PV plants is exceedingly high. Therefore, once these plants are installed, the primary focus shifts to continuously harnessing peak power from the installed PV systems[6]. Developing pump systems powered directly by PV necessitates the utilization of MPPT (Maximum Power Point Tracking) algorithms to operate under varying irradiation levels and extract the maximum power from the PV systems[7][8][9].

https://doi.org/10.25077/jnte.v13n1.1177.2024

This paper undertakes a comprehensive comparative analysis of existing research focused on photovoltaic (PV) systems serving as direct pump drivers for induction motors, eliminating the need for batteries. The study effectively classifies these PV systems into two distinct model types: the two-stage and single-stage models. The classification is based on the power transformation processes from PV to the motor load. The outcomes of this analytical investigation, succinctly presented in tabular form, offer a detailed comparative assessment of these diverse models.

The discussion in this paper is structured around elucidating the concept of a PV-driven pump system, classifying models, explaining the two-stage model, describing the single-stage model, and comparing the two models based on MPPT algorithms. Additionally, the discussion encompasses a comparison of motor controls, a comparison of DC-link capacitors, and an analysis of the comparative study. It concludes with a summary.

PV SYSTEMS SUPPLYING MOTOR LOAD

Several studies discuss models of PV systems supplying induction motor loads commonly used as pump drivers [10]. PV systems generate the electrical energy source. The PV system must be connected to an electrical load to generate energy. In this context, the induction motor for pump driving serves as the electrical load. The electrical energy generated by PV systems is not constant but rather determined by the intensity of sunlight and the connected electrical load. The maximum power from the PV systems at each sunlight intensity level is attained by regulating the power consumption of the motor load. A Voltage Source Inverter (VSI) is employed to control the motor's power consumption [11].

Considering that the electrical load can be adjusted, PV manufacturers can calculate the maximum power points for each sunlight level applied to the PV system. In practical implementation, tracking the maximum power points generated by the PV at different sunlight levels requires the use of an electrical load [12]. A convenient method for laboratory requirements in this tracking process involves using a variable resistor (rheostat) [13]. Utilizing a rheostat can adjust the magnitude of the power-consuming load. The rheostat's resistance value will be varied to track the maximum power, as illustrated in Figure 1.

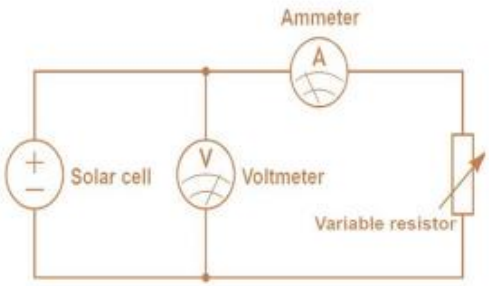

Figure 1. The Concept of Maximum Power Tracking Circuit Using a Variable Resistor [13]

The analogy concept using a rheostat for tracking maximum power production by PV can illustrate a PV system directly driving a pump motor. In this system without using batteries, the power tracking process is executed through the motor load. The motor load consumes electrical power as required to ensure the PV produces power at its maximum point. To enable this electric motor to consume adjustable electrical power, a system block capable of regulating the power consumed by the motor is necessary. The concept of this system involves power tracking and regulation of power consumption for the pump motor load.

Since the pump characteristics are centrifugal, the power consumed is directly proportional to the pump speed. The power consumed by the motor can be controlled by varying the voltage and frequency of the motor [14]. Variations in V/f (voltage-to-frequency ratio) will determine speed differences and impact power consumption by the motor [15]. The determination of motor speed will be based on load torque and PV output voltage[3]. The torque graph in a parabolic form concerning voltage and power, considering PV power production, is illustrated in Figure 2.

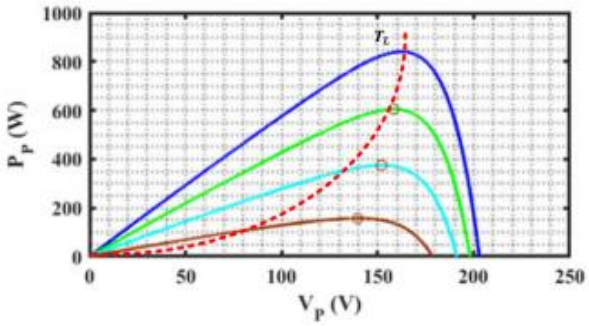

Figure 2. Parabolic Torque Graph Concerning Voltage and Electrical Power [3]

CLASSIFICATION OF PV SYSTEMS SUPPLYING MOTOR LOAD

The classification of models from various studies related to PV systems powering pump motors has been conducted directly in this analytical study. This study categorizes models into two types. The first type is the two-stage model, where the power tracking process and consumption regulation of the motor load are carried out separately. The second type is the single-stage model, where the power tracking process and power consumption regulation to the load are integrated into a single unit.

Two-Stage Model Of Pv System Supplying Pump Motor

The two-stage model of the PV system supplying the pump motor is generally depicted in Figure 3. It's termed as a two-stage PV model because the power production tracking by the PV system and the power consumption regulation by the load are handled by two distinct functional modules. The converter module functions to track the power produced by the PV through the application of MPPT algorithms [9]. Meanwhile, the inverter module regulates the power consumption to the motor load based on input from the converter.

Several studies have been conducted on this two-stage model with the aim of enhancing the maximum power that the load can utilize. Study [3] regulates the induction module, which consists of two power conditioning units, namely the DC-DC boost

https://doi.org/10.25077/jnte.v13n1.1177.2024

converter and the three-phase voltage source inverter. The power tracking process is carried out using the Boost converter, while vector control is employed to provide effective motor speed. A BLDC motor is utilized as the load in study [16]. The use of a high-gain DC-DC boost converter is implemented as a substitute for the conventional converter to increase voltage gain [17].

PI control is employed to regulate the DC link voltage and motor speed [18]. Field-oriented control strategy is utilized to govern the motor speed [19]. Batteries are added in parallel with the DC link as additional storage [20]. MPPT is controlled using the P&O algorithm to supply power to the inverter [21]. An LC filter is added after the inverter to facilitate motor control [22]. The implementation of a neuro-fuzzy controller (ANFIS) is applied in the MPPT process [23]. Predictive torque and flux control (PTC) are used to control the motor [24]. Motor control is carried out with space vector pulse width modulation [25].

In this model, the operation is carried out by integrating an inverter into the DC-DC converter with a separate control scheme for the inverter. The inverter provides the desired frequency and voltage to the load, while the DC-link serves as the available DC for the inverter module. To achieve enhanced dynamic performance, the required DC-link voltage is maintained through a voltage controller. In fluctuating irradiance conditions, the output current from the PV is determined by the DC-link voltage. Therefore, based on the PV output current, the load current also varies.

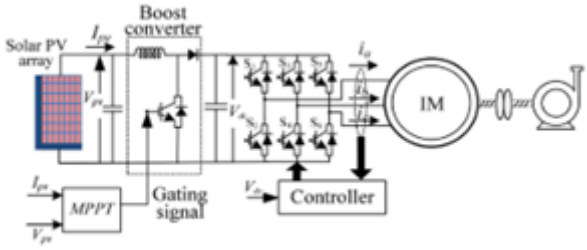

Figure 3. Two-Stage model of the PV system supplying the pump motor [26]

The general operational components of this model consist of PV, the Converter Block, DC-Link Capacitor, Inverter Block, and the motor load driving the pump, as depicted in Figure 3. The PV serves as the power generator, while the Converter is controlled by the MPPT algorithm control system to generate power at its maximum point. The DC-Link Capacitor functions to stabilize voltage changes in the converter's output, enhancing the system's robustness, reliability, and stability. A three-phase voltage source inverter (VSI) is utilized to supply power to the motor load [27]. The types of control for this VSI include Scalar Control (v/f control), Vector Control, and Direct Torque Control (DTC) [28].

The function of the Converter Block in the Two-Stage Model

In this two-stage model, maximum power tracking is performed in the converter block. The maximum power produced by the PV for each irradiance level must be tracked. Failure to track this can result in the PV user not harnessing the maximum energy from the utilized PV. The MPPT controller, containing the MPPT algorithm [29][30], will govern the converter in the maximum power tracking process. What is controlled here is the output voltage of the converter. The discussion on maximum power tracking in this two-stage model is detailed in the research [26].

The characteristics of the relationship between power and PV voltage are illustrated in Figure 4 [31]. In each condition, the operating point depends on the impedance of the load connected to the PV [32][33]. A DC-DC converter is utilized to track the operating point on the PV curve [34]. There are numerous algorithms in the literature for maximum power point tracking. The most basic one is Perturb and Observe [35], where step changes are applied to the reference voltage or duty ratio of the converter, and the output voltage is monitored [36]. However, it faces some issues during changes in irradiance. The Incremental Conductance (IC) method works more effectively during dynamic changes in irradiance[37].

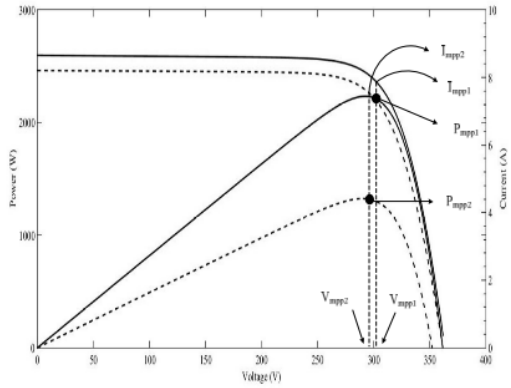

Figure 4. Two-Stage model of the PV system supplying the pump motor [26]

On the right side of the MPP, the slope is negative, while on the left side, the slope is positive. At the point where the PV transfers the maximum power, the slope is zero. With changes in irradiance, at the MPP, I_{PV} changes drastically, while V_{PV} remains almost constant. Considering a power equation and differentiating it with respect to voltage, the relationship between an IC and conductance for different parts of the curve is obtained as follows.

$$P_{PV} = V_{PV} \times I_{PV} \tag{1}$$

$$\frac{dP_{PV}}{dV_{PV}} = I_{PV} + V_{PV} * \frac{dI_{PV}}{dV_{PV}} = 0 \tag{2}$$

$$\frac{dI_{PV}}{dV_{PV}} = -\frac{I_{PV}}{V_{PV}} \tag{3}$$

On the right side of the MPP, the slope is negative, indicating that an increase in voltage at the converter results in a decrease in the output power from the PV.

$$\frac{\mathrm{dI_{PV}}}{\mathrm{dV_{PV}}} < -\frac{\mathrm{I_{PV}}}{\mathrm{V_{PV}}} \tag{4}$$

And on the left side, the slope is positive, signifying that an increase in voltage at the converter results in an increase in the output power from the solar panel.

$$\frac{\mathrm{dI_{PV}}}{\mathrm{dV_{PV}}} > -\frac{\mathrm{I_{PV}}}{\mathrm{V_{PV}}} \tag{5}$$

At the MPP, the slope is zero, meaning that changes in the increase in voltage at the converter do not alter the power generated by the solar panel.

$$\frac{dI_{PV}}{dV_{PV}} = -\frac{I_{PV}}{V_{PV}} \quad (6)$$

The maximum power tracking algorithm is illustrated in Figure 5. In this algorithmic process, the duty ratio of the converter output is increased based on the power tracking obtained from current and voltage sensor readings from the solar panel.

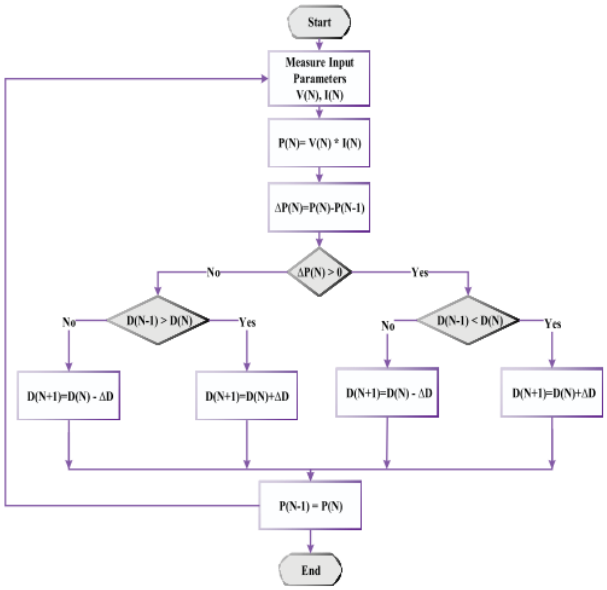

Figure 5. MPPT Algorithm to control the converter output in the two-stage model [38].

The function of the Inverter Block in the Two-Stage Model

The inverter block in this two-stage model operates independently of the MPPT control. This inverter uses the voltage on the DC-link as a reference voltage to determine the power supply to the motor. The block diagram illustrating the speed command as a function of motor speed variation concerning changes in PV output power is depicted in Figure 6 [18]. The inverter control employs the V/f method. The V/f control algorithm generates logic switching for the VSI using SPWM (Sinusoidal Pulse Width Modulation). If the voltage on the DC-link capacitor is higher than the controller's reference value, the controller increases the reference speed given to the V/f control, and vice versa.

In the study [17], it is mentioned that the relationship between load torque and motor speed is nonlinear. The motor load torque is proportional to the motor speed. Hence, the fundamental formula is as follows [3].

$$T_L = m_l \omega_1^2 \quad (7)$$

Where T_L is the load torque, m_l is the load constant, ω_1 is the motor speed.

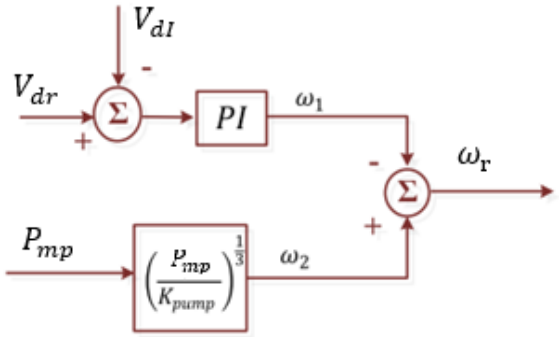

Figure 6. Control system on the inverter to regulate motor power consumption [18]

The power consumed by the motor corresponds to the output power from the solar panel, given by the following equation.

$$\eta P_{mp} = T_L \omega_1 \quad (8)$$

Where η is the efficiency of the power conversion system, P_{mp} is the maximum power produced by the solar panel. By substituting the equations above, the equation is obtained,

$$\eta P_{mp} = m_l \omega_1^3 \quad (9)$$

$$\omega_1 = \sqrt[3]{P_{mp}/m_n} \quad (10)$$

Where $m_n = (m_1/\eta)$. Furthermore, the speed based on the DC-link voltage conditions (ω_1) varies depending on voltage variations. However, the variation has a range of 0.7 to 0.9 times the open-circuit voltage only for MPP tracking. Voltage error can be measured from the DC-link and reference voltage as [26], [27].

$$V_{dI}(k) = V_{dr}(k) - V_d(k) \quad (11)$$

Where V_{dI} is the DC-link voltage, V_{dr} is the DC reference voltage, and V_d is the measured voltage. The speed (ω_2) for the DC-link voltage error is as follows:

$$\omega_2(k) = \omega_2(k-1) + K_{pd}[V_{dl}(k) - V_{dl}(k-1)] + K_{pi} V_{dl}(k) \quad (12)$$

Where K_{pd} and K_{pi} are proportional and integral, respectively. Thus, the reference speed of the drive motor is as follows:

$$\omega_r = \omega_1 + \omega_2 \quad (13)$$

Thus, the reference frequency of the motor is obtained as follows:

$$f^* = \frac{1}{2\pi}(\omega_r) \quad (14)$$

Therefore, for every voltage value provided by the DC-link capacitor to the inverter, a frequency value is obtained, ensuring that the specified V/f is satisfied.

The DC-Link in the Two-Stage Model

The DC-Link capacitor is positioned between the converter and the inverter [39]. As the converter and inverter blocks have separate controls, this capacitor serves as the voltage reference

https://doi.org/10.25077/jnte.v13n1.1177.2024

for the inverter. In the study [18], the DC-Link capacitance C_{dc} is determined based on the equation

$$C_{dc} = \frac{6\alpha VIt}{V_{dc}^{*2} - V_{dc_1}^2} \quad (15)$$

Where V_{dc}^{*2} is the reference DC bus voltage, while $V_{dc_1}^2$ is the lowest acceptable voltage during transient processes and is chosen to be 375V, α is the overloading factor (1.2), V and I are the voltage and current of the motor phase, and t is the duration of the transient. Meanwhile, the minimum voltage required by the DC-Link capacitor is obtained from the following equation:

$$\text{m} \times \frac{V_{DC}}{2\sqrt{2}} = \frac{V_{L-L}}{\sqrt{3}} \quad (16)$$

Where m is the modulation index, and V_{L-L} is the line voltage used in the motor. Therefore,

$$V_{DC} = \frac{2\sqrt{2}}{\sqrt{3}} \times 400 = 653\text{V} \quad (17)$$

It is the voltage required when the modulation index is 1 [4] .

Single-Stage Model Of Pv System Supplying Pump Motor

The single-stage PV system model is generally depicted in Figure 7. It is termed as a single-stage PV model because, in this PV system supplying electrical power to the battery-less motor, it only utilizes the inverter module without incorporating the converter block, as observed in the two-stage model. The voltage generated by the PV is not pre-regulated but is directly used as an input to the inverter block. Subsequently, the inverter determines the output voltage and frequency to be supplied to the motor.

Various studies utilizing this single-stage model incorporate different techniques to enhance the maximum power that can be utilized by motor loads. Research [40] employs a vector control scheme to regulate induction motors, aiming to enhance the reliability of PV systems. The phase current of induction motors is estimated from the DC link current using a modified SVM technique [41]. An incremental-conductance-based maximum power point tracking algorithm is utilized to control voltage source inverters [42].

The power tracking process of PV is conducted through the control of BLDC motors [43]. The use of DC buses can eliminate the need for a dc-dc converter in PV systems to supply power to motors [44]. Frequency variables are harnessed to control induction motors [45]. A combination of variable stepped incremental conductance and constant voltage methods is employed to develop a fast tracking algorithm for generating optimal voltage and frequency references in inverters [46].

In more detail, the single-stage model in a PV system supplying power to the battery-less pump consists of the PV, DC-Link Capacitor, Inverter, and motor. The PV functions as the power generator. The DC-Link Capacitor stabilizes changes in the output voltage from the PV. The MPPT algorithm is applied to directly control the inverter in the maximum power tracking process. The inverter is used to supply power to the motor load.

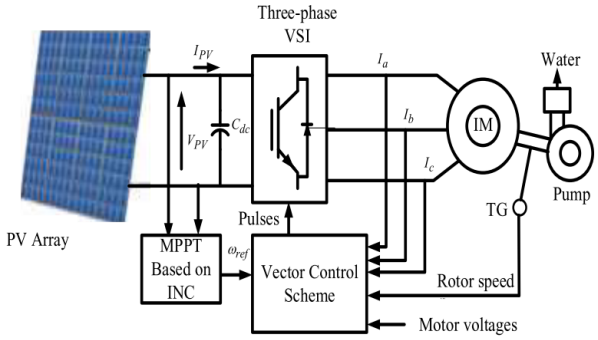

Figure 7. Single-Stage Model of the PV system supplying the pump motor [40]

The function of the Inverter Block in the Single-Stage Model

In the single-stage model, the tracking of power produced by the PV is carried out by the inverter module. In this tracking process, voltage and current sensors gather real-time data from the PV output. This voltage and current data are processed by the MPPT algorithm. The decisions generated by this algorithm determine the speed of the motor driven by the inverter. The motor speed, in turn, impacts the power consumption of the motor.

In the study [47], the control algorithm initially initializes the value of the modulation index m_a to its minimum value. This m_a value is used to calculate the base frequency of the modulation signal m_a.

$$f_{\text{mod}} = \begin{cases} \frac{m_a \times 50}{0.866} & \text{for } m_a \leqslant 0.866 \\ 50 & \text{for } m_a > 0.866 \end{cases} \quad (18)$$

The MPPT algorithm senses the instantaneous PV voltage $\boldsymbol{V_{pv}}$ and PV current $\boldsymbol{I_{pv}}$, then calculates the power $\boldsymbol{P_{pv}}$. This value is stored as the previous value. The current value and the previous value are compared to determine the operating region on the P-V curve.

$$\frac{P_{pv}(n) - P_{pv}(n-1)}{V_{pv}(n) - V_{pv}(n-1)} < 0 \text{ then } m_a = m_a + \Delta m_a \quad (19)$$

$$\frac{P_{pv}(n) - P_{pv}(n-1)}{V_{pv}(n) - V_{pv}(n-1)} > 0 \text{ then } m_a = m_a - \Delta m_a \quad (20)$$

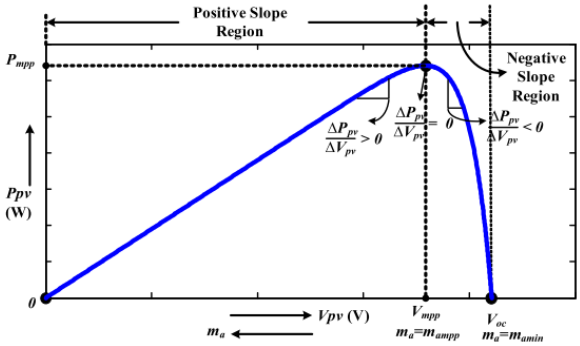

Figure 8. The process of maximum power point tracking by adjusting the modulation index in the inverter block [47]

In determining this motor speed, there are other parameters required as well to ensure that the inverter block provides an

appropriate output. These additional parameters include the current flowing into the motor, motor voltage, and the motor speed at that moment. These parameters serve as references for the inverter. For instance, when the MPPT algorithm provides a speed reference value to the inverter, the inverter must also take these parameters into account. This allows the inverter to determine the voltage and frequency to be supplied to the motor. Research studies such as [41] [10] simplify these parameters for a more concise approach.

Moreover, [46] the motor speed is determined by the MPPT algorithm to achieve the maximum power that the PV can produce. In other words, the primary focus in implementing PV to supply the motor is to track the maximum power from the PV rather than setting a speed reference. Thus, open-loop speed control is used in this implementation. The V/f speed control determines the voltage and frequency values for the PWM generator based on the speed reference.

The flowchart of the MPPT algorithm is illustrated in Figure 8. Here, two methods are employed: Incremental Conductance (IC) and Constant Voltage (CV). The process begins with the CV method to expedite the operation, but as the PV voltage decreases towards the MPP voltage (0.80 of Voc), the IC method comes into play. The step size of the IC method varies depending on the dP/dV value to enhance performance.

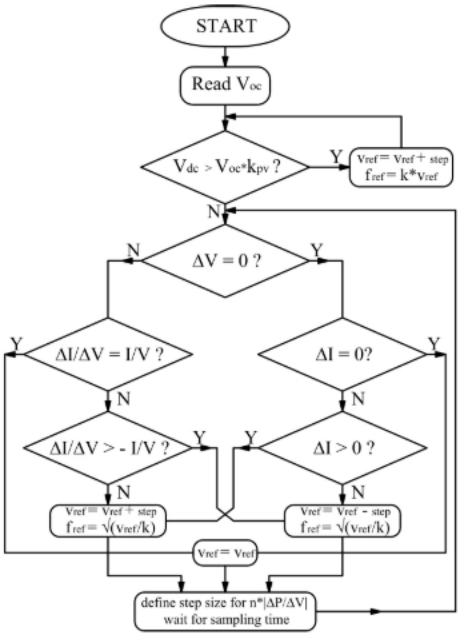

Figure 9. MPPT Algorithm to control the inverter output in the single-stage model [46]

The DC-Link Capacitor in the Single-Stage Model

In this single-stage model, the DC-Link capacitor is positioned between the PV and the inverter block. This capacitor serves as a temporary energy storage for PV, ensuring that during changes in light intensity levels, the power tracking process using the inverter does not undergo spontaneous changes but rather has stored energy to cover any variations. This allows the MPPT algorithm to have time to handle reductions in load power consumption. Additionally, this DC-Link capacitor also functions as a stabilizer for the ripples caused by motor operations. The larger the capacitor used, the more effective its performance.

The ripple current is formulated as follows [43]:

$$\boldsymbol{i_c = i_{pv} - i_{dc}} \tag{21}$$

Where $\boldsymbol{i_{pv}}$ is the current generated by PV at MPP, i_{dc} is the DC-link current entering the inverter, and the ripple current i_c will be significant if i_{dc} is zero. The capacitor value needed for minimal ripple current approaching zero is

$$c = \frac{i_{c,max}}{f_{sw} \times \Delta v_{pv}} \tag{22}$$

In the study [48], the capacitor value is determined based on the analysis of the ripple current that the capacitor will handle, where i_c is given by:

$$i_c = i_{pv} - i_{inv} \tag{23}$$

Where i_{pv} is the current supplied by the PV source, $i_{inv}$is the current consumed by the inverter. Thus, the required capacitance value is given by:

$$C_{pv} = \frac{i_{c,max}}{f_s \Delta V_{pv}} \tag{24}$$

Where f_s is the semiconductor switching frequency, and ΔV_{pv} is the ripple.

In the study [40], the formula for the minimum capacitance of a capacitor that must be used is formulated as:

$$C_{dc} \geq \frac{P}{2\omega V_{dc} \Delta v_{dc}} \tag{25}$$

where V_{dc} is the reference voltage of the VSI. P is the required power. Furthermore, ω is the angular frequency in rad/sec, while Δv_{dc} is the ripple voltage to be handled. Based on their research, after inputting the data, the size of the capacitor is obtained as:

$$C_{dc} \geq \frac{10*746}{2*2*pi*50*600*1} \tag{26}$$

$$C_{dc} \geq 1.9798\text{e} - 04 \tag{27}$$

METHODS

A comparative analysis between the two types of PV system models supplying pump motors, namely two-stage, and single-stage, can be broadly examined in terms of MPPT control[19], motor power consumption regulation, and the role of the DC-link capacitor.

Comparison in MPPT Control

The differences in the MPPT power tracking flowcharts between the two-stage model [26] and the single-stage model [40] are illustrated in Figures 10 and 11. This flowchart can be divided into two main blocks. The first block represents the process of determining the position of tracking the maximum power point, while the second block involves the regulation of load power consumption[49]. The position-tracking determination process

https://doi.org/10.25077/jnte.v13n1.1177.2024

exhibits similarities in both types of models. All types of MPPT algorithms can be implemented in both models[50][51].

The distinguishing factor lies in the regulation of load power consumption. In the two-stage model, the adjustment of motor power consumption is not directly performed; instead, it merely involves providing DC output voltage. On the other hand, in the single-stage model, the load power consumption is directly regulated, controlling the power supplied to the motor. In summary, the overall difference between the single-stage and two-stage models in the power tracking control process is depicted in Figures 10 and 11.

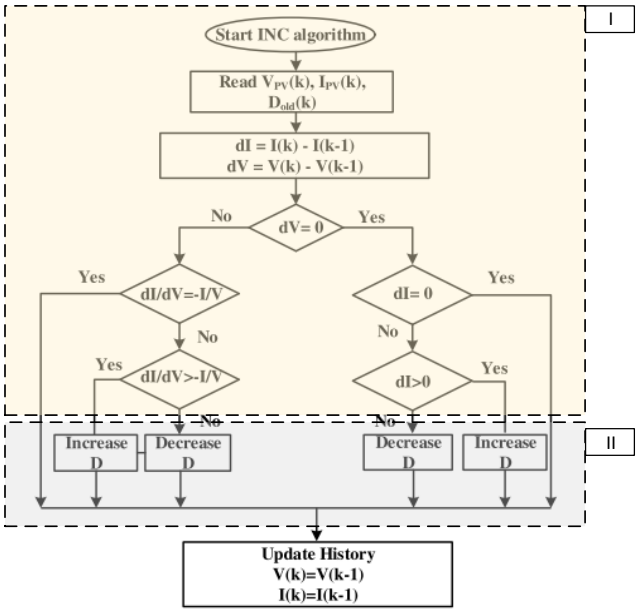

Figure 10. MPPT Block in the Two-Stage Model

In the two-stage model, power regulation towards the load, in this case, an electric motor, is not directly conducted. Instead, it requires the assistance of an inverter block for power regulation towards the load. In this maximum power tracking process, the converter is controlled by the MPPT algorithm to generate a specific voltage. This resultant DC voltage is converted into three-phase AC voltage by the inverter to supply power to the pump motor load

The magnitude of the three-phase AC voltage output by the inverter depends on the DC voltage provided by the converter block. The higher the DC voltage supplied, the greater the AC voltage produced by the inverter. Here, the role of the inverter block is to facilitate electrical power conversion.

In the single-stage model, the power consumption regulation process is performed by the inverter. The MPPT algorithm controls the inverter in the maximum power tracking process by adjusting the inverter output voltage, either increasing or decreasing it. This inverter output voltage determines the corresponding frequency

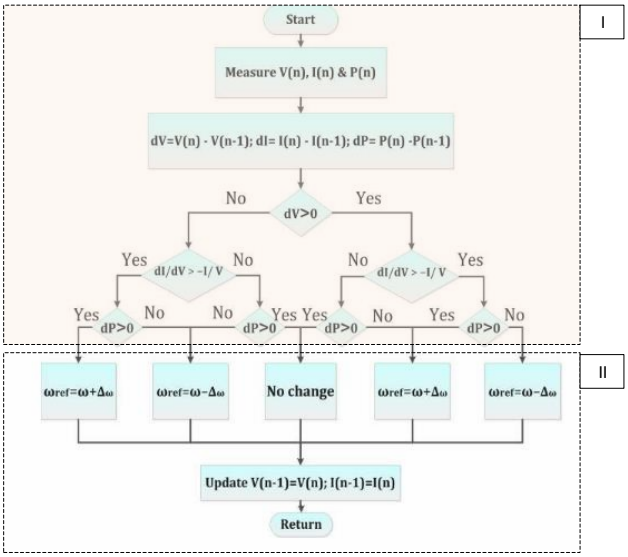

Figure 11. MPPT Block in the Single-Stage Mode

Comparison in Motor Power Consumption Regulation

The Two-Stage model employs separate controls for the MPPT process and the motor power consumption regulation. In contrast, the Single-Stage model integrates both MPPT and motor power consumption control into a single process. In the Two-Stage model, the regulation of motor power consumption is entirely dependent on the DC-link capacitor, which serves as the voltage source for the inverter. The determination of motor power consumption is based on this DC-link capacitor. On the other hand, in the Single-Stage model, motor power consumption is determined through the power tracking process facilitated by the MPPT algorithm

Since the Two-Stage model features separate controls, regulating power consumption to the motor typically involves using a PI Controller in the inverter. In this case, the voltage on the DC link serves as the basis for determining the motor speed. The voltage on the DC link is utilized as a reference in the inverter control. Additionally, this DC link voltage serves as a power tracker for the converter, as it does not directly control the inverter.

The Single-Stage model employs the directive of the maximum power tracking algorithm to control the motor speed. The parameters used to increase motor speed in this context are in the form of modulation index or frequency parameters [47][46]. Subsequently, for this processing, a vector scheme control is employed [40].

Comparison in the Use of DC Link Capacitors

Comparison of DC-link Capacitor Usage between Two-Stage and Single-Stage Models is primarily based on the capacitor's main function. In the two-stage model, it serves as a temporary energy storage for the power produced by PV, which is then directed to the motor through the inverter. On the other hand, in the single-stage model, its primary purpose is to mitigate ripple voltage resulting from fluctuations in power production by PV. Functionally, the required capacity value for the two-stage model will be smaller compared to the single-stage model.

In the two-stage model, the determination of the capacitor does not involve the motor load behavior, thus not considering the

frequency in determining the capacity of the DC Link capacitor. In the study by [26] , the DC-link capacitor functions to provide sufficient energy during transient events, such as a decrease in radiation and an increase in load. Its value is calculated as follows:

$$\frac{1}{2}C_{DC}\left[V_{DC}^{*_2} - V_{DC1}^2\right] = 3\alpha VIt \quad (24)$$

In this equation, $V_{DC}^{*_2}$ represents the DC bus voltage, while V_{DC1}^2 refers to the lowest acceptable voltage during transients. Furthermore, α denotes the overloading factor, and t is the duration of the transient.

In a single-stage configuration, the motor load behavior is considered, thereby involving the motor frequency. In the study [40], the formula for the minimum capacitance of a capacitor that must be utilized is formulated as follows:

$$C_{dc} \geq \frac{P}{2\omega V_{dc}\Delta v_{dc}} \quad (25)$$

Where V_{dc} represents the reference voltage of the VSI. P denotes the required power. Furthermore, ω stands for the angular frequency in rad/sec, while Δv_{dc} signifies the handled ripple voltage.

RESULTS AND DISCUSSION

This study categorizes standalone PV-powered motor systems models into two models: the two-stage model and the single-stage model. A comparative analysis of these two models is presented in tabular form, as shown in Table 1. The study's analysis of the maximum power tracking process between the two-stage and single-stage models reveals a significant difference. The two-stage model employs a separate system, whereas the single-stage model utilizes an integrated system.

In the process of maximum power point tracking (MPPT) by the photovoltaic (PV) system supplying power to the motor, load consumption regulation and power production monitoring are two crucial aspects. As this PV-powered motor system operates standalone without using batteries, the regulation of power consumption by the motor load must be directly controlled. The two-stage model employs two functional blocks: the converter function block and the inverter function block. The converter function block is utilized to implement the MPPT algorithm, while the inverter function block is used to control the motor's power consumption. On the other hand, the single-stage model integrates the MPPT algorithm and the control of motor power consumption within the inverter function block, eliminating the need for a separate converter function block.

All types of MPPT algorithms can be applied to both of these models. The use of MPPT algorithms in the two-stage model aims to regulate the output voltage from the converter function block. This voltage regulation is achieved through adjusting the duty cycle based on the voltage and current generated by the PV system. The voltage regulation significantly impacts the output voltage and current of the solar panels. Meanwhile, in the single-stage model, the purpose of employing MPPT algorithms is to determine the motor speed or modulation index. The motor speed directly influences the voltage and current output from the PV system.

Table 1. Comparison of Two-Stage Model with Single-Stage Model

Parameters	**Two-Stage Model**	**Single-Stage Model**
Maximum Power Point Tracking System	Separate	Integrated
Power Tracking Process	Performed by converter	Performed by inverter
Converter Module	Required	Not required
Inverter Module	Required	Required
MPPT Control Output	DC Voltage	Motor Speed
DC Link Capacitor	Required	Required
DC Link Role	Reference Voltage	Power Production Fluctuations
DC-Link Capacity	Voltage	Motor Speed
Motor Load Power Consumption Adjustment Process	In the Inverter	In the Inverter
Types of MPPT Algorithms Applicable	All algorithms	All algorithms
Scalar Control	Can be used	Preferred for use
Vector Control	Preferred for use	Can be used
Motor Speed Reference	Preferred for use	Can be used
Close Loop	Preferred for use	Can be used
Open Loop	Can be used	Preferred for use

The DC-link capacitor plays a crucial role in this standalone PV system supplying power to the motor. This component provides the system with the necessary time to adjust voltage settings during fluctuations in sunlight intensity or when the load increases in power consumption. In the two-stage model, the DC-link capacitor serves as the inverter's reference voltage in determining the motor's power consumption. When determining this DC link's capacity, the voltage input to the inverter is the parameter used. In the single-stage model, the capacity of the DC link is determined based on the motor speed.

https://doi.org/10.25077/jnte.v13n1.1177.2024

In motor control, the motor speed can be regulated using scalar control and vector control. Both types of control can be applied in both models. However, the single-stage model commonly employs scalar control in PV system studies for motor supply. This is because the motor control process directly utilizes MPPT algorithms. Scalar control does not necessitate feedback from the motor. The MPPT algorithm utilizes the tracked power as a reference to determine the motor speed. Conversely, the two-stage model tends to favor vector control for regulating motor speed. This inclination stems from the inverter block having separate control from MPPT in the two-stage model.

CONCLUSION

The results of the analytical study conducted on research related to PV systems supplying power to pump motor loads have led to the classification of these PV systems into two distinct models. The first model is the two-stage, and the second model is the single-stage. Between these two models, the two-stage model exhibits higher stability due to the separation of the power tracking process from the PV system and the regulation of the pump motor load consumption. The power tracking process involves the converter module, while the load consumption regulation process occurs in the inverter module. In the single-stage model, both the power tracking process and the control of pump motor load consumption are integrated into a single process. In the single-stage model, the inverter module receives input voltage with significant fluctuations, impacting the utilization of the DC-link capacitor. The single-stage model requires a capacitor with a larger capacity to stabilize fluctuations resulting from changes in voltage from the PV.

REFERENCES

[1] Anil Kumar Saini and Ashish Kumar Dubey, "Performance Analysis of Single Phase Induction Motor with Solar PV Array for water Pumping System," *Int. J. Eng. Res.*, vol. V6, no. 04, 2017, doi: 10.17577/ijertv6is040567.

[2] C. Soenen *et al.*, "Comparison of Tank and Battery Storages for Photovoltaic Water Pumping," *Energies*, vol. 14, no. 9, pp. 5–7, 2021.

[3] A. Narendra, V. Naik N, A. K. Panda, and R. K. Lenka, "Solar PV fed FSVSI based Variable Speed IM Drive using ASVM Technique," *Eng. Sci. Technol. an Int. J.*, vol. 40, p. 101366, 2023, doi: 10.1016/j.jestch.2023.101366.

[4] B. G. Reshma Raj O, "Solar PV Fed Induction Motor Driven Water Pumping System using High Gain Converter," *Irjet*, vol. 8, no. 7, pp. 3601–3610, 2021.

[5] S. Bhattacharjee and P. K. Nayak, "PV-pumped energy storage option for convalescing performance of hydroelectric station under declining precipitation trend," *Renew. Energy*, vol. 135, pp. 288–302, 2019, doi: 10.1016/j.renene.2018.12.021.

[6] A. Faizal and B. Setyaji, "Desain Maximum Power Point Tracking (MPPT) pada Panel Surya Menggunakan Metode Sliding Mode Control," *J. Sains, Teknol. dan Ind.*, vol. 14, no. 1, pp. 22–31, 2016.

[7] O. S. S. Hussian, H. M. Elsayed, and M. A. Moustafa Hassan, "Fuzzy Logic Control for a Stand-Alone PV System with PI Controller for Battery Charging Based on Evolutionary Technique," *Proc. 2019 10th IEEE Int. Conf. Intell. Data Acquis. Adv. Comput. Syst. Technol. Appl. IDAACS 2019*, vol. 2, pp. 889–894, 2019, doi: 10.1109/IDAACS.2019.8924269.

[8] T. Radjai, L. Rahmani, S. Mekhilef, and J. P. Gaubert, "Implementation of a modified incremental conductance MPPT algorithm with direct control based on a fuzzy duty cycle change estimator using dSPACE," *Sol. Energy*, vol. 110, pp. 325–337, 2014, doi: 10.1016/j.solener.2014.09.014.

[9] M. A. G. De Brito, L. Galotto, L. P. Sampaio, G. De Azevedo Melo, and C. A. Canesin, "Evaluation of the main MPPT techniques for photovoltaic applications," *IEEE Trans. Ind. Electron.*, vol. 60, no. 3, pp. 1156–1167, 2013, doi: 10.1109/TIE.2012.2198036.

[10] H. Kraiem, "Sensorless torque and flux control of induction motor fed by photovoltaic system," *Meas. Control (United Kingdom)*, vol. 55, no. 5–6, pp. 454–462, 2022, doi: 10.1177/00202940221104869.

[11] M. M. Elkholy and A. Fathy, "Optimization of a PV fed water pumping system without storage based on teaching-learning-based optimization algorithm and artificial neural network," *Sol. Energy*, vol. 139, pp. 199–212, 2016, doi: 10.1016/j.solener.2016.09.022.

[12] K. Y. Chou, S. T. Yang, and Y. P. Chen, "Maximum power point tracking of photovoltaic system based on reinforcement learning," *Sensors (Switzerland)*, vol. 19, no. 22, 2019, doi: 10.3390/s19225054.

[13] A. Ajitha *et al.*, "Underwater performance of thin-film photovoltaic module immersed in shallow and deep waters along with possible applications," *Results Phys.*, vol. 15, no. October, p. 102768, 2019, doi: 10.1016/j.rinp.2019.102768.

[14] R. Gafar, X. Sun, and T. Abozead, "Three-phase AC Induction Motor Speed Control Based on Variable Speed Driver," *Makara J. Technol.*, vol. 26, no. 2, pp. 54–58, 2022, doi: 10.7454/mst.v26i2.1523.

[15] S. N. Patrialova, D. H. Wardhana, L. P. Rahayu, and T. Agasta, "The Characteristic of Variable Frequency Drive for Water Flow Control in the SFC Plant," *IPTEK J. Eng.*, vol. 7, no. 1, p. 6, 2021, doi: 10.12962/j23378557.v7i1.a8415.

[16] A. Ammar, K. Hamraoui, M. Belguellaoui, and A. Kheldoun, "Performance Enhancement of Photovoltaic Water Pumping System Based on BLDC Motor under Partial Shading Condition," *Eng. Proc.*, vol. 14, no. 1, p. 22, 2022, doi: 10.3390/engproc2022014022.

[17] Z. M. S. Elbarbary, K. M. Cheema, S. F. Al-Gahtani, and R. A. El-Sehiemy, "High gain chopper supplied from PV system to fed synchronous reluctance motor drive for pumping water application," *Sci. Rep.*, vol. 12, no. 1, pp. 1–15, 2022, doi: 10.1038/s41598-022-19671-x.

[18] G. H. K. Varma, V. R. Barry, and R. K. Jain, "A Total-Cross-Tied-Based Dynamic Photovoltaic Array Reconfiguration for Water Pumping System," *IEEE Access*, vol. 10, pp. 4832–4843, 2022, doi: 10.1109/ACCESS.2022.3141421.

[19] T. Hamdi and A. Toumi, "Sliding mode controller with fuzzy supervisor for MPPT of Photovoltaic Pumping system," *Int. J. Power Electron. Drive Syst.*, vol. 14, no. 3, pp. 1639–1650, 2022.

[20] A. Loubna, T. Riad, and M. Salima, "Standalone photovoltaic array fed induction motor driven water pumping system," *Int. J. Electr. Comput. Eng.*, vol. 10, no. 5, pp. 4534–4542, 2020, doi: 10.11591/ijece.v10i5.pp4534-4542.

[21] A. A. S. Esmeail, S. Oncu, and N. Altin, "An MPPT Controlled Three Phase PV Supplied Water Pumping System," *Proc. 13th Int. Conf. Electron. Comput. Artif. Intell. ECAI 2021*, no. April 2022, pp. 1–6, 2021, doi: 10.1109/ECAI52376.2021.9515018.

[22] C. Ghizlane, Z. Massaq, A. Abounada, and M.

Mabrouki, "Speed control of induction motor driving a pump supplied by a photovoltaic array," *Int. J. Renew. Energy Res.*, vol. 10, no. 1, pp. 237–242, 2020, doi: 10.20508/ijrer.v10i1.10320.g7859.

[23] H. Hamdi, C. Ben Regaya, and A. Zaafouri, "A sliding-neural network control of induction-motor-pump supplied by photovoltaic generator," *Prot. Control Mod. Power Syst.*, vol. 5, no. 1, pp. 1–17, 2020, doi: 10.1186/s41601-019-0145-1.

[24] B. Talbi, F. Krim, T. Rekioua, S. Mekhilef, A. Laib, and A. Belaout, "A high-performance control scheme for photovoltaic pumping system under sudden irradiance and load changes," *Sol. Energy*, vol. 159, no. November 2017, pp. 353–368, 2018, doi: 10.1016/j.solener.2017.11.009.

[25] H. Bouzeria, C. Fetha, T. Bahi, I. Abadlia, Z. Layate, and S. Lekhchine, "Fuzzy Logic Space Vector Direct Torque Control of PMSM for Photovoltaic Water Pumping System," *Energy Procedia*, vol. 74, pp. 760–771, 2015, doi: 10.1016/j.egypro.2015.07.812.

[26] B. Singh, U. Sharma, and S. Kumar, "Standalone Photovoltaic Water Pumping System Using Induction Motor Drive with Reduced Sensors," *IEEE Trans. Ind. Appl.*, vol. 54, no. 4, pp. 3645–3655, 2018, doi: 10.1109/TIA.2018.2825285.

[27] B. Singh and S. Shukla, "Induction motor drive for PV water pumping with reduced sensors," *IET Power Electron.*, vol. 11, no. 12, pp. 1903–1913, 2018, doi: 10.1049/iet-pel.2017.0856.

[28] V. T. Akhila and S. Arun, "Review of Solar PV Powered Water Pumping System Using Induction Motor Drive," *IOP Conf. Ser. Mater. Sci. Eng.*, vol. 396, no. 1, 2018, doi: 10.1088/1757-899X/396/1/012047.

[29] H. D. Liu, C. H. Lin, K. J. Pai, and C. M. Wang, "A GMPPT algorithm for preventing the LMPP problems based on trend line transformation technique," *Sol. Energy*, vol. 198, no. November 2019, pp. 53–67, 2020, doi: 10.1016/j.solener.2020.01.049.

[30] M. Arsalan, R. Iftikhar, I. Ahmad, A. Hasan, K. Sabahat, and A. Javeria, "MPPT for photovoltaic system using nonlinear backstepping controller with integral action," *Sol. Energy*, vol. 170, no. January, pp. 192–200, 2018, doi: 10.1016/j.solener.2018.04.061.

[31] E. Durán, J. M. Andújar, J. M. Enrique, and J. M. Pérez-Oria, "Determination of PV generator I-V/P-V characteristic curves using a DC-DC converter controlled by a virtual instrument," *Int. J. Photoenergy*, vol. 2012, no. January, 2012, doi: 10.1155/2012/843185.

[32] S. Khunchan and B. Wiengmoon, "Method to determine the single curve IV characteristic parameter of solar cell," *J. Phys. Conf. Ser.*, vol. 1144, no. 1, 2018, doi: 10.1088/1742-6596/1144/1/012012.

[33] T. Suntio, T. Messo, A. Aapro, J. Kivimäki, and A. Kuperman, "Review of PV generator as an input source for power electronic converters," *Energies*, vol. 10, no. 8, 2017, doi: 10.3390/en10081076.

[34] A. M. Noman, H. S. Sheikh, A. F. Murtaza, S. Z. Almutairi, M. H. Alqahtani, and A. S. Aljumah, "Maximum Power Point Tracking Algorithm of Photovoltaic Array through Determination of Boost Converter Conduction Mode," *Appl. Sci.*, vol. 13, no. 14, 2023, doi: 10.3390/app13148033.

[35] R. Alik, A. Jusoh, and T. Sutikno, "A review on Perturb and Observe maximum power point tracking in photovoltaic system," *Telkomnika (Telecommunication Comput. Electron. Control.*, vol. 13, no. 3, pp. 745–751, 2015, doi: 10.12928/telkomnika.v13i3.1439.

[36] E. M., I. M., and A. I., "High Step up DC-DC Converter Fed from Photovoltaic System," *Int. J. Comput. Appl.*, vol. 139, no. 3, pp. 6–13, 2016, doi: 10.5120/ijca2016909427.

[37] S. André, F. Silva, S. Pinto, and P. Miguens, "Novel Incremental Conductance Feedback Method with Integral Compensator for Maximum Power Point Tracking: A Comparison Using Hardware in the Loop," *Appl. Sci.*, vol. 13, no. 7, 2023, doi: 10.3390/app13074082.

[38] N. Genc, "PV based V/F controlled induction motor drive for water pumping," *Int. J. Tech. Phys. Probl. Eng.*, vol. 12, no. 4, pp. 103–108, 2020.

[39] M. A. Memon, "Sizing of dc-link capacitor for a grid connected solar photovoltaic inverter," *Indian J. Sci. Technol.*, vol. 13, no. 22, pp. 2272–2281, 2020, doi: 10.17485/ijst/v13i22.406.

[40] M. Abd El Sattar, K. Ahmed, A. AboZied, and A. Diab, "Adaptive MPPT of Water Photovoltaic Pumping System Based on Vector Controlled Induction Motor Drives," *J. Adv. Eng. Trends*, vol. 41, no. 2, pp. 261–274, 2021, doi: 10.21608/jaet.2021.47871.1065.

[41] S. Shukla and B. Singh, "Single-Stage PV-Grid Interactive Induction Motor Drive with Improved Flux Estimation Technique for Water Pumping with Reduced Sensors," *IEEE Trans. Power Electron.*, vol. 35, no. 12, pp. 12988–12999, 2020, doi: 10.1109/TPEL.2020.2990833.

[42] S. Shukla and B. Singh, "Single-Stage PV Array Fed Speed Sensorless Vector Control of Induction Motor Drive for Water Pumping," *IEEE Trans. Ind. Appl.*, vol. 54, no. 4, pp. 3575–3585, 2018, doi: 10.1109/TIA.2018.2810263.

[43] J. M. Mumthas A, "Simulation and Analysis of Single Stage Solar PV fed Brushless DC motor for Water Pumping," *Int. J. Innov. Res. Electr. Electron. Instrum. Control Eng.*, vol. 1, no. 2, pp. 107–112, 2018.

[44] R. Antonello, C. Costabeber, Alessandror, F. Tinazzi, and M. Zigliotto, "Energy-Efficient Autonomous Solar Synchronous Motors," *IEEE Trans. Ind. Electron.*, vol. 64, no. 1, pp. 43–51, 2017.

[45] T. S. R. R. Eddy and B. A. Nuradha, "Modeling and Simulation of Solar PV Wind Hybrid System for Induction Motor Drive Application," *Int. J. Innov. Sci. Eng. Technol.*, vol. 04, no. 09, pp. 1655–1660, 2016.

[46] S. Ozdemir, N. Altin, I. Sefa, and G. Bal, "PV supplied single stage mppt inverter for induction motor actuated ventilation systems," *Elektron. ir Elektrotechnika*, vol. 20, no. 5, pp. 116–122, 2014, doi: 10.5755/j01.eee.20.5.7111.

[47] C. Ramulu, P. Sanjeevikumar, R. Karampuri, S. Jain, A. H. Ertas, and V. Fedak, "A solar PV water pumping solution using a three-level cascaded inverter connected induction motor drive," *Eng. Sci. Technol. an Int. J.*, vol. 19, no. 4, pp. 1731–1741, 2016, doi: 10.1016/j.jestch.2016.08.019.

[48] G. Jain, V. K. Arun Shankar, and S. Umashankar, "Modelling and simulation of solar photovoltaic fed induction motor for water pumping application using perturb and observer MPPT algorithm," *2016 Int. Conf. Energy Effic. Technol. Sustain. ICEETS 2016*, no. April, pp. 250–254, 2016, doi: 10.1109/ICEETS.2016.7582935.

[49] S. A. Rizzo and G. Scelba, "ANN based MPPT method for rapidly variable shading conditions," *Appl. Energy*, vol. 145, no. May, pp. 124–132, 2015, doi: 10.1016/j.apenergy.2015.01.077.

[50] H. A. Sher, A. F. Murtaza, A. Noman, K. E. Addoweesh, K. Al-Haddad, and M. Chiaberge, "A New Sensorless Hybrid MPPT Algorithm Based on Fractional Short-Circuit Current Measurement and P&O MPPT," *IEEE Trans. Sustain. Energy*, vol. 6, no. 4, pp. 1426–1434, 2015, doi: 10.1109/TSTE.2015.2438781.

https://doi.org/10.25077/jnte.v13n1.1177.2024

[51] Y. Li, Z. Tang, Z. Zhu, and Y. Yang, "A novel MPPT circuit with 99.1% tracking accuracy for energy harvesting," *Analog Integr. Circuits Signal Process.*, vol. 94, no. 1, pp. 105–115, 2018, doi: 10.1007/s10470-017-1079-z.

NOMENCLATURE

V	Voltage
f	Frequency
I_{PV}	Photovoltaic Current
P_{PV}	Photovoltaic Power
V_{PV}	Photovoltaic Voltage
dI_{PV}	Derivative of the photovoltaic current
dV_{PV}	Derivative of the photovoltaic voltage
P_{mp}	Power comsumed by motor
T_L	Load torque
P_{mp}	Power comsumed by motor
P_{mp}	Power comsumed by motor
ω	Motor speed
η	Efficiency of the power conversion
C	Capacitance
m_a	Modulation